Ocean Engineering 248 (2022) 110686

Contents lists available at ScienceDirect

Ocean Engineering

journal homepage: www.elsevier.com/locate/oceaneng

Anti-disturbance leader–follower synchronization control of marine vessels for underway replenishment based on robust exact differentiators

Wentao Wu [a,b], Zhouhua Peng [a,*], Dan Wang [a], Lu Liu [a], Nan Gu [a]

[a] School of Marine Electrical Engineering, Dalian Maritime University, Dalian 116026, China
[b] SJTU Yazhou Bay Institute of Deepsea Science and Technology, Sanya 572024, China

ARTICLE INFO

Keywords:
Underway replenishment
Robust exact differentiator
Finite-time stability
Anti-disturbance control

ABSTRACT

This paper considers the leader–follower synchronization control of under-actuated marine vessels for underway replenishment. An integrated guidance and control method is presented to achieve the underway replenishment operations despite of unknown model uncertainties, external disturbances, and unknown velocities of the leader vessel. Specifically, a velocity observer based on a robust exact differentiator (RED) is firstly designed to estimate the unknown velocity of the leader vessel. Next, a finite-time light-of-sight guidance law based on the velocity observer is developed to synchronize the follower vessels with the leader vessel. Then, two disturbance observers based on REDs are designed to estimate the total disturbances composed of model uncertainties and external disturbances at the kinetic level. With the aid of the RED-based disturbance observers, an anti-disturbance nonlinear control law is presented to track the desired guidance signals in finite time. The tracking errors of the closed-loop system are proved to be ultimately uniformly bounded via Lyapunov stability theory. Finally, an example is utilized to illustrate the effectiveness of the proposed anti-disturbance synchronization control method for multiple under-actuated marine vessels.

1. Introduction

Underway replenishment operations are of critical importance in case that it is impractical or impossible to return to base to replenish supplies such as fuel, food, parts, or personnel due to mission requirements (Kyrkjebø, 2007; Skejic et al., 2009). It is essential for long-term military and civil missions to shorten port time. As an important means to ensure the sustained navigation and operation of marine vessels, underway replenishment is a fundamental problem and has drawn intensive research interests. In general, the control objective of underway replenishment operation is to coordinate the motion of the supply and replenished vessels in a leader–follower configuration (Breivik et al., 2008; Kyrkjebø, 2007).

During the past few years, control of marine vessels for underway replenishment has been widely studied in the literature, and a number of effective methods are proposed (Belleter and Pettersen, 2017; Bondhus and Pettersen, 2005; Gierusz and Miller, 2016; Kyrkjebø, 2015; Skejic et al., 2009; Kyrkjebø et al., 2007; Liu et al., 2018a). Specifically, in Belleter and Pettersen (2017), a constant bearing guidance method with known leader velocity is proposed to assure the synchronized motion of the marine vessels. In Bondhus and Pettersen (2005), an observer-controller scheme is presented to synchronize two ships by using position-yaw information only. In Gierusz and Miller (2016), a kinematic controller based on model predictive method is proposed to track the generated reference trajectory for approaching the leader vessel. In Kyrkjebø (2015), kinematic and dynamic observers are designed to estimate missing velocity and acceleration state information required in coordination control. In Skejic et al. (2009), a unified seakeeping and maneuvering model of two advancing ships is proposed based on a two-time scales and modular concept relevant for calm water. The interaction forces and moments between the two ships are estimated by using Newman–Tuck theory. In Kyrkjebø et al. (2007), a leader–follower output feedback synchronization control scheme is presented for the underway replenishment problem by using position measurement only. In this study, the model of the leader ship is not needed. In Liu et al. (2018a), a nonlinear control law based on a dynamic surface control technique and a robust term is proposed. The above works in Belleter and Pettersen (2017), Bondhus and Pettersen (2005), Gierusz and Miller (2016), Kyrkjebø (2015), Skejic et al. (2009), Kyrkjebø et al. (2007) and Liu et al. (2018a) have made significant contributions for underway replenishment operations, whereas the restrictions are as follows. The synchronization controllers in Belleter and Pettersen (2017), Gierusz and Miller (2016), Skejic et al. (2009), Kyrkjebø et al. (2007) and Liu et al. (2018a) is designed by assuming that the vessel velocity is available. The authors in Bondhus

* Corresponding author.
E-mail address: zhpeng@dlmu.edu.cn (Z. Peng).

https://doi.org/10.1016/j.oceaneng.2022.110686
Received 4 February 2021; Received in revised form 13 January 2022; Accepted 22 January 2022
Available online 12 February 2022

and Pettersen (2005) and Kyrkjebø (2015) present two linear velocity observers to recover the unavailable velocity. Besides, the finite-time synchronization of the follower vessels and the leader vessel fails to be achieved by using the above controllers, which does not have better robustness and transient performance.

Motivated by the above mentioned observations, an anti-disturbance synchronization control method is proposed to achieve the underway replenishment for multiple under-actuated marine vessels with unknown model uncertainties and external disturbances. Firstly, a velocity observer based on robust exact differentiator (RED) is designed to estimate the unavailable velocity of the leader vessel due to the constrains/faults of network or sensor. Based on the RED-based velocity observer, a finite-time light-of-sight (FTLOS) guidance law is developed to synchronize the follower vessels and the leader vessels. Secondly, two disturbance observers based on REDs are proposed to estimate the unknown disturbances in the surge and yaw direction. Based on the proposed observers, a nonlinear anti-disturbance control law is developed. Finally, stability analysis shows that all errors of the closed-loop system are ultimately uniformly bounded, and underway replenishment of multiple marine vessels can be achieved in a finite time via the proposed anti-disturbance synchronization control method. The salient contribution of this paper is summarized as three-holds.

- In contrast to the synchronization guidance methods in Zhang et al. (2017), Liu et al. (2017, 2016, 2020b), Cui et al. (2012), Zheng and Zou (2016), Zheng et al. (2018), Gierusz and Miller (2016), Kyrkjebø (2015), Skejic et al. (2009), Kyrkjebø et al. (2007), He et al. (2022), Ihle et al. (2007) and He et al. (2022), where the leader velocity is available, this paper designs a velocity observer based on RED to estimate the unknown velocity of the leader vessel. With the recovered velocity, an FTLOS guidance law is firstly developed to synchronize multiple marine vessels in a finite time.
- In contrast to the disturbance observers proposed in Wu et al. (2021), Lu et al. (2018, 2020), Cui et al. (2017), Dai et al. (2012), He et al. (2019), Qin et al. (2020), Peng et al. (2020, 2021, 2013), Guo et al. (2019), Bondhus and Pettersen (2005), Liu et al. (2019), Gu et al. (2019), Kyrkjebø (2015) and Jin (2016), the RED-based disturbance observers are devised to estimate the total unknown disturbances composed of model uncertainties and external disturbances, which can enhance the robustness and convergence.
- In contrast to the designed kinetic control laws in Bondhus and Pettersen (2005), Liu et al. (2018b), Wang and Han (2017), Gu et al. (2019, 2020), Peng et al. (2019), Liu et al. (2020a), Xiang et al. (2017) and Chu et al. (2017), the proposed finite-time anti-disturbance control law enables to track the desired guidance velocity in a finite time. Besides, it is proved that all error signals of the proposed closed-loop system are ultimately uniformly bounded in finite-time.

This paper is organized as follows: Section 2 claims the problem formulation. Section 3 provides the design and analysis of anti-disturbance synchronization control method for the underway replenishment system. Section 4 provides a simulation example. Section 5 concludes this paper.

2. Preliminaries and problem formulation

2.1. Preliminaries

The following notations are used in this paper. $\mathbb{R}$, $\mathbb{R}^+$ and $\mathbb{R}^n$ present a real set, a positive real set and a n-dimensional real set, respectively. $(\cdot)^T$ describes the transpose of a vector or a matrix. $|\cdot|$ and $\|\cdot\|$ present the absolute value of a real number and the Euclidean norm of a vector, respectively. $\lambda_{\max}(\cdot)$ and $\lambda_{\min}(\cdot)$ are the maximum and minimum eigenvalue of a symmetric matrix. For a real vector $x \in \mathbb{R}^n$ and a real number $\gamma \in \mathbb{R}$, the symbol $\lceil x \rfloor^\gamma$ is defined as $\lceil x \rfloor^\gamma = [\lceil x_1 \rfloor^\gamma, \ldots, \lceil x_n \rfloor^\gamma]^T$ with $\lceil x_i \rfloor^\gamma = |x_i|^\gamma \mathrm{sign}(x_i)$, where $\mathrm{sign}(x)$ is a sign function.

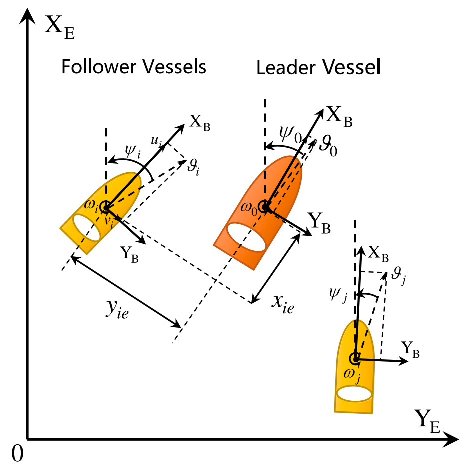

Fig. 1. A geometrical relationship of underway replenishment.

2.2. Lemmas

The following lemmas are used in this paper.

Lemma 1 (*Hong et al., 2001*). *Consider a nonlinear system $\dot{x}(t) = f(x(t))$ with $f(0) = 0$, $x \in \mathbb{R}^n$. Suppose there is a continuously differentiable function $V(x)$ defined in a neighborhood $U_1 \subset \mathbb{R}^n$ of the origin, and there are real numbers $a_1 > 0$ and $0 < \kappa_1 < 1$, such that $V(x)$ is positive definite on U_1 and*

$$\dot{V}(x) + a_1 V^{\kappa_1}(x) \le 0. \tag{1}$$

Then, the zero solution of system is finite-time stable. Depending on initial state $x(0) = x_0$, the settling time is given by $T \le V^{1-\kappa_1}(x_0)/a_1(1-\kappa_1)$ for all x_0 in some open neighborhood of the origin.

Lemma 2 (*Moulay and Perruquetti, 2006*). *Considering a nonlinear system $\dot{x}(t) = f(x(t))$ satisfying $f(0) = 0$, $x \in U_2 \subset \mathbb{R}^n$, suppose that there exists a continuous Lyapunov function V(x), real numbers $a_2 > 0$, $a_3 > 0$, and $0 < \kappa_2 < 1$ such that*

$$\dot{V}(x) + a_2 V(x) + a_3 V^{\kappa_2}(x) \le 0. \tag{2}$$

Then, the system is finite-time stable. For any given initial time t_0, the settling time $T = t_0 + \dfrac{1}{a_2(1-\kappa_2)} \ln\left(\dfrac{a_2 V_1^{1-\kappa_2}(x(t_0)) + a_3}{a_3}\right)$.

2.3. Problem formulation

The motion of a marine vessel can be expressed in the north-east-down frame {N} and the body-fixed frame {B} shown in Fig. 1. Consider an underway replenishment system consisted of a leader vessel and N follower vessels. The kinematic model of the leader vessel is presented as follows (Fossen, 2011)

$$\begin{cases} \dot{x}_0 = \vartheta_0 \cos\psi_0, \\ \dot{y}_0 = \vartheta_0 \sin\psi_0, \\ \dot{\psi}_0 = \omega_0, \end{cases} \tag{3}$$

where $x_0 \in \mathbb{R}$, $y_0 \in \mathbb{R}$ and $\psi_0 \in \mathbb{R}$ are the position and heading angular of the leader vessel in {N}; $\vartheta_0 = \sqrt{u_0^2 + v_0^2}$ is the total velocity of the leader vessel with u_0 and v_0 being the surge and sway velocity. The velocities u_0 and v_0 of the leader vessel may not be available. ω_0 is the heading angular velocity in {B}.

Let $x_i \in \mathbb{R}$, $y_i \in \mathbb{R}$ and $\psi_i \in \mathbb{R}$ denote the position and heading angular of the ith follower marine vessel in {N}; $\vartheta_i = \sqrt{u_i^2 + v_i^2}$ presents the total speed, where u_i and v_i are the surge and sway velocity in {B},

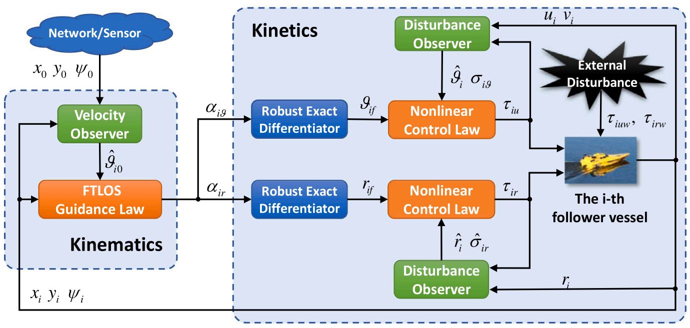

Fig. 2. The leader–follower synchronization control architecture of the ith marine vessel.

respectively; r_i is the yaw angular velocity; $\beta_{id} = \dot{\beta}_i$ presents the time derivative of the sideslip angle in {B} with $\beta_i = \mathrm{atan2}(v_i,\ u_i)$. Thus, the motion dynamics of the ith follower vessel can be described as (Fossen, 2011)

$$\begin{cases} \dot{x}_i = \vartheta_i \cos\psi_i, \\ \dot{y}_i = \vartheta_i \sin\psi_i, \\ \dot{\psi}_i = r_i + \beta_{id}, \end{cases} \tag{4}$$

and

$$\begin{cases} m_{iu}\dot{u}_i = f_{iu}(u_i, v_i, r_i, t) + \tau_{iu}(t) + \tau_{iuw}(t), \\ m_{iv}\dot{v}_i = f_{iv}(u_i, v_i, r_i, t) + \tau_{ivw}(t), \\ m_{ir}\dot{r}_i = f_{ir}(u_i, v_i, r_i, t) + \tau_{ir}(t) + \tau_{irw}(t), \end{cases} \tag{5}$$

where m_{iu}, m_{iv} and m_{ir} are the inertia terms of the ith vessel; $f_{iu}(\cdot)$, $f_{iv}(\cdot)$ and $f_{ir}(\cdot)$ are the unknown functions including Coriolis terms, damping terms and unmodeled dynamics; τ_{iuw}, τ_{ivw} and τ_{irw} are the unknown external time-varying disturbance owing to wind, waves and currents; τ_{iu} and τ_{ir} are the control input torques.

Noting that $u_i = \vartheta_i \cos\beta_i$, the kinetic model (5) can be represented as follows

$$\begin{cases} m_{iu}\dot{\vartheta}_i = f_{iu}(\cdot) + \tau_{iu} + \tau_{iuw} + 2m_{iu}\vartheta_i \sin^2(\frac{\beta_i}{2}) + m_{iu}\vartheta_i \sin(\beta_i)\beta_{id}, \\ m_{ir}\dot{r}_i = f_{ir}(\cdot) + \tau_{ir} + \tau_{irw}(t). \end{cases} \tag{6}$$

Before stating the control objective, define two kinematic tracking errors in $\{B\}$ as follows

$$\begin{cases} x_{ie} = (x_i - x_0)\cos\psi_0 + (y_i - y_0)\sin\psi_0 - \delta_{ix}, \\ y_{ie} = -(x_i - x_0)\sin\psi_0 + (y_i - y_0)\cos\psi_0 - \delta_{iy}, \end{cases} \tag{7}$$

where $x_{ie} \in \mathbb{R}$ and $y_{ie} \in \mathbb{R}$ are the along-track errors and cross-track errors in {B}; δ_{ix} and δ_{iy} are the predefined distances to guarantee the safety of underway replenishment operations. The control objective of this paper is to develop an anti-disturbance synchronization control method of the under-actuated follower ships model described with (4) and (5) such that

$$\begin{cases} \lim_{t\to\infty} |x_{ie}| \le \varepsilon_{ix}, \\ \lim_{t\to\infty} |y_{ie}| \le \varepsilon_{iy}, \end{cases} \tag{8}$$

where $\varepsilon_{ix} \in \mathbb{R}^+$ and $\varepsilon_{iy} \in \mathbb{R}^+$ are small constants.

3. Design and analysis

In this section, an integrated guidance and control method is presented to achieve the underway replenishment operations despite of unknown model uncertainties, external disturbances, and unknown velocities of the leader vessel. The architecture of the proposed synchronization controller includes a finite-time kinematic guidance law and a finite-time kinetic control law shown in Fig. 2.

3.1. FTLOS guidance law

In this part, firstly, a RED-based velocity observer is designed to estimate the total velocity of the leader vessel. Next, a kinematic guidance law based on FTLOS is developed to provide the desired synchronization commands with the estimated velocity. Finally, the stability of each error subsystem in the kinematic level is analyzed via the Lyapunov stability theory.

(i) RED-based velocity observer

Taking the derivative of (7) with (3) and (4), it renders that

$$\begin{cases} \dot{x}_{ie} = \vartheta_i \cos(\psi_i - \psi_0) + \omega_0(y_{ie} + \delta_{iy}) + \vartheta_{i0}, \\ \dot{y}_{ie} = \vartheta_i \sin(\psi_i - \psi_0) - \omega_0(x_{ie} + \delta_{ix}), \end{cases} \tag{9}$$

where $\vartheta_{i0} = -\vartheta_0$.

To recover the unavailable velocity ϑ_0 for the follower marine vessels, a velocity observer based on RED is designed as follows (Davila et al., 2009)

$$\begin{cases} \dot{\hat{x}}_{ie} = -\gamma_{i1}\lceil \hat{x}_{ie} - x_{ie} \rfloor^{\frac{1}{2}} + \hat{\vartheta}_{i0} + \vartheta_i \cos(\psi_i - \psi_0) + \omega_0(y_{ie} + \delta_{iy}), \\ \dot{\hat{\vartheta}}_{i0} = -\gamma_{i2}\lceil \hat{x}_{ie} - x_{ie} \rfloor^{0}, \end{cases} \tag{10}$$

where $\hat{x}_{ie}$ and $\hat{\vartheta}_{i0}$ are the estimations of x_{ie} and ϑ_{i0}, respectively; $\gamma_{i1} \in \mathbb{R}^+$ and $\gamma_{i2} \in \mathbb{R}^+$ are the observer gains.

Define the estimated errors $\tilde{x}_{ie} = \hat{x}_{ie} - x_{ie}$ and $\tilde{\vartheta}_{i0} = \hat{\vartheta}_{i0} - \vartheta_{i0}$. Along (9) and (10), the time derivative of $\tilde{x}_{ie}$ and $\tilde{\vartheta}_{i0}$ can be presented as follows

$$\begin{cases} \dot{\tilde{x}}_{ie} = -\gamma_{i1}\lceil \tilde{x}_{ie} \rfloor^{\frac{1}{2}} + \tilde{\vartheta}_{i0}, \\ \dot{\tilde{\vartheta}}_{i0} = -\gamma_{i2}\lceil \tilde{x}_{ie} \rfloor^{0} - \dot{\vartheta}_{i0}. \end{cases} \tag{11}$$

Letting $z_{i1} = [\tilde{x}_{ie},\ \tilde{\vartheta}_{i0}]^T$ and $\xi_{i1} = \left[\lceil \tilde{x}_{ie} \rfloor^{\frac{1}{2}},\ \tilde{\vartheta}_{i0}\right]^T$, Eq. (11) can be represented as

$$\dot{\xi}_{i1} = A_{i1}\xi_{i1}/|\xi_{i1}^{(1)}| + B_{i1}\dot{\vartheta}_{i0}, \tag{12}$$

where $\xi_{i1}^{(1)} = \lceil \tilde{x}_{ie} \rfloor^{\frac{1}{2}}$, $A_{i1} = \begin{bmatrix} -\frac{1}{2}\gamma_{i1} & \frac{1}{2} \\ -\gamma_{i2} & 0 \end{bmatrix}$ and $B_{i1} = \begin{bmatrix} 0 \\ -1 \end{bmatrix}$.

To analyze the stability of the subsystem (11), the following assumption is needed.

Assumption 1. For the leader vessel, the time derivative of ϑ_{i0} is uniformly bounded, such that for all $t > t_0$: $|\dot{\vartheta}_{i0}| \le \bar{\vartheta}_{i0}$ with $\bar{\vartheta}_{i0}$ being a positive constant.

Applying the transformed term $\breve{\vartheta}_{i0} = |\xi_{i1}^{(1)}|\dot{\vartheta}_{i0}$, it yields that $\breve{\vartheta}_{i0}$ satisfies $|\breve{\vartheta}_{i0}(t,\ \xi_{i1})| \le \bar{\vartheta}_{i0}|\xi_{i1}^{(1)}|$, that is $\zeta_{i1}(\breve{\vartheta}_{i0},\ \xi_{i1}) = -\breve{\vartheta}_{i0}^2(t,\ \xi_{i1}) + \bar{\vartheta}_{i0}^2\xi_{i1}^{(1)2} \ge 0$. Then, (12) can rewritten as

$$\dot{\xi}_{i1} = \frac{1}{|\xi_{i1}^{(1)}|}\left(A_{i1}\xi_{i1} + B_{i1}\breve{\vartheta}_{i0}\right). \tag{13}$$

Noting that A_{i1} is a Hurwitz matrix, the robust stability analysis can be performed through

$$\begin{bmatrix} A_{i1}^T P_{i1} + P_{i1}A_{i1} + \epsilon_{i1}P_{i1} + \bar{\vartheta}_{i0}^2 C_{i1}^T C_{i1} & P_{i1}B_{i1} \\ B_{i1}^T P_{i1} & -1 \end{bmatrix} < 0, \tag{14}$$

where $C_{i1} = [1 \quad 0]$.

The stability of the subsystem (11) can be given as below.

Lemma 3. *Suppose that there exist a symmetric and positive definite matrix $P_{i1} = P_{i1}^T > 0$ such that (14) or equivalently, the Algebraic Riccati Equation*

$$A_{i1}^T P_{i1} + P_{i1}A_{i1} + \bar{\vartheta}_{i0}^2 C_{i1}^T C_{i1} + P_{i1}B_{i1}B_{i1}^T P_{i1} = -Q_{i1} \tag{15}$$

is satisfied with $Q_{i1} > 0$. In this case, the error signal z_{i1} of subsystem (11) can converge in finite time to the origin for all $\dot{\vartheta}_{i0}$ under Assumption 1.

Proof. Construct a Lyapunov function $V_1(z_{11},\dots,z_{N1})$ as

$$V_1(z_{11},\dots,z_{N1})=\sum_{i=1}^{N}\xi_{i1}^TP_{i1}\xi_{i1}. \tag{16}$$

Along (13), the time derivative of V_1 renders that

$$\begin{aligned}\dot V_1&=\sum_{i=1}^{N}\frac{1}{|\xi_{i1}^{(1)}|}\begin{bmatrix}\xi_{i1}\\ \breve\vartheta_{i0}\end{bmatrix}^T\begin{bmatrix}A_{i1}^TP_{i1}+P_{i1}A_{i1} & P_{i1}B_{i1}\\ B_{i1}^TP_{i1} & 0\end{bmatrix}\begin{bmatrix}\xi_{i1}\\ \breve\vartheta_{i0}\end{bmatrix}\\ &\le\sum_{i=1}^{N}\frac{1}{|\xi_{i1}^{(1)}|}\left\{\begin{bmatrix}\xi_{i1}\\ \breve\vartheta_{i0}\end{bmatrix}^T\begin{bmatrix}A_{i1}^TP_{i1}+P_{i1}A_{i1} & P_{i1}B_{i1}\\ B_{i1}^TP_{i1} & 0\end{bmatrix}\begin{bmatrix}\xi_{i1}\\ \breve\vartheta_{i0}\end{bmatrix}+\zeta_{i1}\right\}.\end{aligned} \tag{17}$$

Using (14) and (15), $\dot V_1$ follows that

$$\begin{aligned}\dot V_1&\le\sum_{i=1}^{N}\frac{1}{|\xi_{i1}^{(1)}|}\left\{\begin{bmatrix}\xi_{i1}\\ \breve\vartheta_{i0}\end{bmatrix}^T\begin{bmatrix}A_{i1}^TP_{i1}+P_{i1}A_{i1} & P_{i1}B_{i1}\\ B_{i1}^TP_{i1} & -1\end{bmatrix}\begin{bmatrix}\xi_{i1}\\ \breve\vartheta_{i0}\end{bmatrix}\right.\\ &\qquad\left.+\begin{bmatrix}\xi_{i1}\\ \breve\vartheta_{i0}\end{bmatrix}^T\begin{bmatrix}\bar\vartheta_{i0}^2C_{i1}^TC_{i1} & P_{i1}B_{i1}\\ B_{i1}^TP_{i1} & -1\end{bmatrix}\begin{bmatrix}\xi_{i1}\\ \breve\vartheta_{i0}\end{bmatrix}\right\}\\ &\le\sum_{i=1}^{N}-\frac{1}{|\xi_{i1}^{(1)}|}\xi_{i1}^TQ_{i1}\xi_{i1}\le\sum_{i=1}^{N}-\chi_{i1}(P_{i1})(\xi_{i1}^TP_{i1}\xi_{i1})^{\frac12}\\ &\le -l_1V_1^{\frac12}(z_{11},\dots,z_{N1}),\end{aligned} \tag{18}$$

where $l_1=\min\{\chi_{11}(P_{11}),\dots,\chi_{N1}(P_{N1})\}$ with

$$\chi_{i1}(P_{i1})=\frac{\lambda_{\min}(Q_{i1})\lambda_{\min}^{\frac12}(P_{i1})}{\lambda_{\max}(P_{i1})}$$

being a scalar depending on the selection of Q_{i1} matrix.

Applying to Lemma 1, the subsystem (11) is finite-time stable. And the estimated errors $\tilde x_{ie}$ and $\tilde\vartheta_{i0}$ can converge to zero in finite time T_1 satisfying $|\tilde x_{ie}|\le\bar x_{ie}$ and $|\tilde\vartheta_{i0}|\le\bar\vartheta_{i0}$ with $\bar x_{ie}\in\mathbb{R}^+$ and $\bar\vartheta_{i0}\in\mathbb{R}^+$ being upper bounds of errors. The time T_1 for (11) meets

$$T_1\le\frac{2}{l_1}V_1^{\frac12}\left(z_{11}(t_0),\dots,z_{N1}(t_0)\right), \tag{19}$$

where $z_{11}(t_0),\dots,z_{N1}(t_0)$ are the initial state at time t_0. □

(ii) FTLOS guidance law

Define the tracking errors $\vartheta_{ie}=\vartheta_i-\vartheta_{if}$ and $q_{i\vartheta}=\vartheta_{if}-\alpha_{i\vartheta}$ with $\alpha_{i\vartheta}$ and ϑ_{if} being the desired velocity signal and the filtered signal of $\alpha_{i\vartheta}$ for follower ships. Then, the position error dynamics (9) can be written as follows

$$\begin{cases}\dot x_{ie}=\alpha_{i\vartheta}+\vartheta_{ie}+q_{i\vartheta}-2\vartheta_i\sin^2\left(\dfrac{\psi_i-\psi_0}{2}\right)+\vartheta_{i0}+\omega_0(y_{ie}+\delta_{iy}),\\ \dot y_{ie}=\vartheta_i\sin(\alpha_{i\psi}-\psi_0+\beta_i)+\varrho_i-\omega_0(x_{ie}+\delta_{ix}),\end{cases} \tag{20}$$

where $\varrho_i=\vartheta_i\sin(\psi_i-\psi_0)-\vartheta_i\sin(\alpha_{i\psi}-\psi_0+\beta_i)$.

The predictor-based LOS guidance law (Liu et al., 2016) and ESO-based guidance law (Liu et al., 2017) aim to estimate the unknown sideslip angle. In addition, the finite-time estimation and control cannot be achieved. In this paper, a FTLOS guidance law is proposed such that the faster convergence of cross-tracking error. Motivated by REDs and finite-time control method (Davila et al., 2009; Jin, 2018), the FTLOS guidance law is proposed as follows

$$\begin{cases}\alpha_{i\vartheta}=-k_{i1}^dx_{ie}-k_{i2}^d\rho_{ix}+2\vartheta_i\sin^2\left(\dfrac{\psi_i-\psi_0}{2}\right)-\hat\vartheta_{i0},\\ \alpha_{i\psi}=\operatorname{atan2}\left(-\dfrac{y_{ie}+k_{i3}^d\rho_{iy}}{\Delta_i}\right)+\psi_0-\beta_i,\end{cases} \tag{21}$$

where k_{i1}^d, k_{i2}^d, and k_{i3}^d are the positive designed control constants; $\Delta_i\in\mathbb{R}^+$ is a look ahead distance. ρ_{ix} and ρ_{iy} are constructed as

$$\begin{aligned}\rho_{ix}&=\begin{cases}\lceil x_{ie}\rfloor^{\frac12}, & |x_{ie}|\ge\iota_{ix},\\ x_{ie}/\iota_{ix}^{-\frac12}, & |x_{ie}|<\iota_{iy}.\end{cases}\\ \rho_{iy}&=\begin{cases}\lceil y_{ie}\rfloor^{\frac12}, & |y_{ie}|\ge\iota_{iy},\\ y_{ie}/\iota_{iy}^{-\frac12}, & |y_{ie}|<\iota_{iy},\end{cases}\end{aligned} \tag{22}$$

where ι_{ix} and ι_{iy} are small positive constants.

Remark 1. By using the constructed terms ρ_{ix} and ρ_{iy}, the continuity of the FTLOS guidance law can be ensured. From (22), we can get that $\rho_{ix}(\iota_{ix}^+)=\lim_{x_{ie}\to\iota_{ix}^+}=|x_{ie}|^{\frac12}$, and $\rho_{ix}(\iota_{ix}^-)=\lim_{x_{ie}\to\iota_{ix}^-}=|x_{ie}|^{\frac12}$ for $x_{ie}>0$, i.e. $\rho_{ix}(\iota_{ix}^+)=\rho_{ix}(\iota_{ix}^-)$. Obviously, it can also obtain that $\rho_{ix}(-\iota_{ix}^+)=\rho_{ix}(-\iota_{ix}^-)$. Then, it concludes that ρ_{ix} is continuous. Similarly, we have $\dot\rho_{ix}(\iota_{ix}^+)=\dot\rho_{ix}(\iota_{ix}^-)$ and $\dot\rho_{ix}(-\iota_{ix}^+)=\dot\rho_{ix}(-\iota_{ix}^-)$, which means that $\dot\rho_{ix}$ is continuous. For ρ_{iy}, the discussion process is omitted due to ρ_{iy} similar to ρ_{ix}.

Next, let $\psi_{ie}=\psi_i-\beta_i-\alpha_{i\psi}$, $r_{ie}=r_i-r_{if}$ and $q_{ir}=r_{if}-\alpha_{ir}$ where α_{ir} is the desired yaw velocity signal for follower ships. r_{if} is the filtered value of α_{ir}. Taking the derivative of ψ_{ie} yields as

$$\dot\psi_{ie}=\alpha_{ir}+r_{ie}+q_{ir}-\dot\alpha_{\psi_i}. \tag{23}$$

To stabilize the dynamics of ψ_{ie}, the desired yaw velocity signal is designed as follows

$$\alpha_{ir}=-k_{i4}^d\psi_{ie}-k_{i5}^d\rho_{i\psi}+\dot\alpha_{i\psi}. \tag{24}$$

where k_{i4}^d, $k_{i5}^d\in\mathbb{R}^+$ are the designed control gains. $\iota_{i\psi}$ meets

$$\rho_{i\psi}=\begin{cases}\lceil\psi_{ie}\rfloor^{\frac12}, & |\psi_{ie}|\ge\iota_{i\psi},\\ \psi_{ie}/\iota_{i\psi}^{-\frac12}, & |\psi_{ie}|<\iota_{i\psi}\end{cases} \tag{25}$$

with $\iota_{i\psi}$ being a small positive constant.

Combining (21), (25), (20), (23), the dynamics of kinematic errors can be devised as follows

$$\begin{cases}\dot x_{ie}=-k_{i1}^dx_{ie}-k_{i2}^d\rho_{ix}+\vartheta_{ie}+q_{i\vartheta}-\tilde\vartheta_{i0}+\omega_0(y_{ie}+\delta_{iy}),\\ \dot y_{ie}=-\underline{\vartheta}_iy_{ie}-\underline{\vartheta}_ik_{i3}^d\rho_{iy}+\varrho_i-\omega_0(x_{ie}+\delta_{ix}),\\ \dot\psi_{ie}=-k_{i4}^d\psi_{ie}-k_{i5}^d\rho_{i\psi}+r_{ie}+q_{ir},\end{cases} \tag{26}$$

where $\underline{\vartheta}_i=\vartheta_i/\sqrt{(y_{ie}+k_{i3}^d\rho_i(y_{ie}))^2+\Delta_i^2}$.

3.2. Kinetic control law

In this part, two REDs are used to obtain the derivative information of the desired guidance signals. Next, two disturbance observers based on REDs are proposed to address the unknown uncertainties and disturbances of marine vessels. With the estimated disturbances, a nonlinear anti-disturbance finite-time control law is developed to track the signals from REDs. Finally, the stability of each error subsystem is proved that tracking error signals can converge to zero in a finite time.

In order to obtain smooth motion profile, the desired guidance signals $\alpha_{i\vartheta}$ and α_{ir} are driven to pass through the following REDs (Levant, 1998)

$$\begin{cases}\dot\vartheta_{if}=-\gamma_{i1}^{\vartheta}\lceil\vartheta_{if}-\alpha_{i\vartheta}\rfloor^{\frac12}+\vartheta_{if}^d,\\ \dot\vartheta_{if}^d=-\gamma_{i2}^{\vartheta}\lceil\vartheta_{if}-\alpha_{i\vartheta}\rfloor^0,\\ \dot r_{if}=-\gamma_{i1}^r\lceil r_{if}-\alpha_{ir}\rfloor^{\frac12}+r_{if}^d,\\ \dot r_{if}^d=-\gamma_{i2}^r\lceil r_{if}-\alpha_{ir}\rfloor^0,\end{cases} \tag{27}$$

where ϑ_{if}^d and r_{if}^d are the estimations of $\dot\alpha_{i\vartheta}$ and $\dot\alpha_{ir}$, respectively; γ_{i1}^{ϑ}, γ_{i2}^{ϑ}, γ_{i1}^r and γ_{i2}^r are the predefined gains with $\gamma_{i1}^{\vartheta}\in\mathbb{R}^+$, $\gamma_{i2}^{\vartheta}\in\mathbb{R}^+$, $\gamma_{i1}^r\in\mathbb{R}^+$ and $\gamma_{i2}^r\in\mathbb{R}^+$.

Assumption 2. In the practical application, the time derivatives of $\alpha_{i\vartheta}$ and α_{ir} is bounded and satisfies $\dot{\alpha}_{i\vartheta} \le \bar{\alpha}_{i\vartheta}$ and $\dot{\alpha}_{ir} \le \alpha_{ir}$ with $\bar{\alpha}_{i\vartheta}$ and $\bar{\alpha}_{ir}$ being positive constants.

According to Levant (1998), the system (27) is finite-time stable under Assumption 2. By selecting the appropriate parameters γ_{i1}^{ϑ}, γ_{i2}^{ϑ}, γ_{i1}^{r} and γ_{i2}^{r}, the estimated error signals $q_{i\vartheta}$ and q_{ir} can converge to small neighborhood of the origin in a finite time and satisfy $|q_{i\vartheta}| \le \bar{q}_{i\vartheta} \in \mathbb{R}^+$ and $|q_{ir}| \le \bar{q}_{ir} \in \mathbb{R}^+$.

(i) The RED-based disturbance observers

To facilitate the design of the kinetic controllers, we rewrite (6) as follows

$$\begin{cases} \dot{\vartheta}_i = \sigma_{i\vartheta}(\cdot) + m_{iu}^{-1}\tau_{iu}, \\ \dot{r}_i = \sigma_{ir}(\cdot) + m_{ir}^{-1}\tau_{ir}, \end{cases} \tag{28}$$

where $\sigma_{i\vartheta}(\cdot)$ and $\sigma_{ir}(\cdot)$ are the unknown functions with $\sigma_{i\vartheta}(\cdot) = m_{iu}^{-1}(f_{iu}(\cdot)+\tau_{iuw}+2m_{iu}\dot{\vartheta}_i \sin^2(\frac{\beta_i}{2})+m_{iu}\vartheta_i \sin(\beta_i)\beta_{id})$ and $\sigma_{ir}(\cdot) = m_{ir}^{-1}(f_{ir}(\cdot)+\tau_{irw})$. The following assumption is needed.

Assumption 3 (*Guo et al., 2016*)**.** The time derivatives of $\sigma_{i\vartheta}$ and σ_{ir} are bounded such that all $t > t_0$: $|\dot{\sigma}_{i\vartheta}(t)| \le \bar{\sigma}_{i\vartheta}$ and $|\dot{\sigma}_{ir}(t)| \le \bar{\sigma}_{ir}$ with $\bar{\sigma}_{i\vartheta}$ and $\bar{\sigma}_{ir}$ being positive constants.

To address the velocity control problem of multiple under-actuated marine vessels under unknown model uncertainties and ocean disturbances, two RED-based observers are proposed to estimate $\sigma_{i\vartheta}(\cdot)$ and $\sigma_{ir}(\cdot)$ as follows

$$\begin{cases} \dot{\hat{\vartheta}}_i = -\gamma_{i3}\lceil \hat{\vartheta}_i - \vartheta_i \rfloor^{\frac{1}{2}} + \hat{\sigma}_{i\vartheta} + m_{iu}^{-1}\tau_{iu}, \\ \dot{\hat{\sigma}}_{i\vartheta} = -\gamma_{i4}\lceil \hat{\vartheta}_i - \vartheta_i \rfloor^{0}, \\ \dot{\hat{r}}_i = -\gamma_{i5}\lceil \hat{r}_i - r_i \rfloor^{\frac{1}{2}} + \hat{\sigma}_{ir} + m_{ir}^{-1}\tau_{ir}, \\ \dot{\hat{\sigma}}_{ir} = -\gamma_{i6}\lceil \hat{r}_i - r_i \rfloor^{0}, \end{cases} \tag{29}$$

where $\hat{\vartheta}_i$, $\hat{\sigma}_{i\vartheta}$, $\hat{r}_i$ and $\hat{\sigma}_{ir}$ denote estimated values of ϑ_i, $\sigma_{i\vartheta}$, r_i and σ_{ir}, respectively; $\gamma_{i3} \in \mathbb{R}^+$, $\gamma_{i4} \in \mathbb{R}^+$, $\gamma_{i5} \in \mathbb{R}^+$ and $\gamma_{i6} \in \mathbb{R}^+$ are predefined observer parameters.

Define estimation errors $\tilde{\vartheta}_i = \hat{\vartheta}_i - \vartheta_i$, $\tilde{\sigma}_{i\vartheta} = \hat{\sigma}_{i\vartheta} - \sigma_{i\vartheta}$, $\tilde{r}_i = \hat{r}_i - r_i$ and $\tilde{\sigma}_{ir} = \hat{\sigma}_{ir} - \sigma_{ir}$. Using (28) and (29), the error dynamics of the subsystem (29) can be expressed as

$$\begin{cases} \dot{\tilde{\vartheta}}_i = -\gamma_{i3}\lceil \tilde{\vartheta}_i \rfloor^{\frac{1}{2}} + \tilde{\sigma}_{i\vartheta}, \\ \dot{\tilde{\sigma}}_{i\vartheta} = -\gamma_{i4}\lceil \tilde{\vartheta}_i \rfloor^{0} - \dot{\sigma}_{i\vartheta}, \\ \dot{\tilde{r}}_i = -\gamma_{i5}\lceil \tilde{r}_i \rfloor^{\frac{1}{2}} + \tilde{\sigma}_{r_i}, \\ \dot{\tilde{\sigma}}_{ir} = -\gamma_{i6}\lceil \tilde{r}_i \rfloor^{0} - \dot{\sigma}_{ir}. \end{cases} \tag{30}$$

Similar to (11), the stability analysis of (30) can be directly given via the following lemma.

Lemma 4. *Suppose that there exist symmetric and positive definite matrices $P_{i2} = P_{i2}^T$ and $P_{i3} = P_{i3}^T$ such that the Algebraic Riccati Equations*

$$\begin{cases} A_{i2}^T P_{i2} + P_{i2}A_{i2} + \bar{\alpha}_{i\vartheta}^2 C_{i2}^T C_{i2} + P_{i2}B_{i2}B_{i2}^T P_{i2} = -Q_{i2}, \\ A_{i3}^T P_{i3} + P_{i3}A_{i3} + \bar{\alpha}_{ir}^2 C_{i3}^T C_{i3} + P_{i3}B_{i3}B_{i3}^T P_{i3} = -Q_{i3} \end{cases} \tag{31}$$

are satisfied with $Q_{i2} > 0$ and $Q_{i3} > 0$, where $z_{i2} = [\tilde{\vartheta}_i,\ \tilde{\sigma}_{i\vartheta}]^T$, $z_{i3} = [\tilde{r}_i,\ \tilde{\sigma}_{ir}]^T$, $B_{i2} = B_{i3} = B_{i1}$, $C_{i2} = C_{i3} = C_{i1}$ and

$$A_{i2} = \begin{bmatrix} -\frac{1}{2}\gamma_{i3} & \frac{1}{2} \\ -\gamma_{i4} & 0 \end{bmatrix} \text{ and } A_{i3} = \begin{bmatrix} -\frac{1}{2}\gamma_{i5} & \frac{1}{2} \\ -\gamma_{i6} & 0 \end{bmatrix}.$$

Therefore, under Assumption 3, the error signals z_{i4} and z_{i5} of subsystem (30) can converge to a small neighborhood of the origin in a finite time.

(ii) Anti-disturbance finite-time control law

Letting $\hat{\vartheta}_{ie} = \hat{\vartheta}_i - \vartheta_{if}$ and $\hat{r}_{ie} = \hat{r}_i - r_{if}$, the time derivatives of $\hat{\vartheta}_{ie}$ and $\hat{r}_{ie}$ can be presented as follows

$$\begin{cases} \dot{\hat{\vartheta}}_{ie} = -\gamma_{i3}\lceil \tilde{\vartheta}_i \rfloor^{\frac{1}{2}} + \hat{\sigma}_{i\vartheta} + m_{iu}^{-1}\tau_{iu} - \dot{\vartheta}_{if}, \\ \dot{\hat{r}}_{ie} = -\gamma_{i5}\lceil \tilde{r}_i \rfloor^{\frac{1}{2}} + \hat{\sigma}_{r_i} + m_{ir}^{-1}\tau_{ir} - \dot{r}_{if}. \end{cases} \tag{32}$$

To stabilize $\hat{\vartheta}_{ie}$ and $\hat{r}_{ie}$, a nonlinear kinetic anti-disturbance control law based on two proposed observer (29) is developed for the follower vessels as follows

$$\begin{cases} \tau_{iu} = m_{iu}(-k_{i1}^c \hat{\vartheta}_{ie} - k_{i2}^c \rho_{i\vartheta} - \hat{\sigma}_{i\vartheta} + \dot{\vartheta}_{if}), \\ \tau_{ir} = m_{ir}(-k_{i3}^c \hat{r}_{ie} - k_{i4}^c \rho_{ir} - \hat{\sigma}_{ir} + \dot{r}_{if}), \end{cases} \tag{33}$$

where $k_{i1}^c \in \mathbb{R}^+$, $k_{i2}^c \in \mathbb{R}^+$, $k_{i3}^c \in \mathbb{R}^+$ and $k_{i4}^c \in \mathbb{R}^+$ are control gains. $\rho_{i\vartheta}$ and ρ_{ir} are defined as

$$\rho_{i\vartheta} = \begin{cases} \lceil \hat{\vartheta}_{ie} \rfloor^{\frac{1}{2}}, & |\hat{\vartheta}_{ie}| \ge \iota_{i\vartheta}, \\ \hat{\vartheta}_{ie}/\iota_{i\vartheta}^{-\frac{1}{2}}, & |\hat{\vartheta}_{ie}| < \iota_{i\vartheta}, \end{cases} \text{ and } \rho_{ir} = \begin{cases} \lceil \hat{r}_{ie} \rfloor^{\frac{1}{2}}, & |\hat{r}_{ie}| \ge \iota_{ir}, \\ \hat{r}_{ie}/\iota_{iy}^{-\frac{1}{2}}, & |r_{ie}| < \iota_{ir}, \end{cases}$$

where $\iota_{i\vartheta}$ and ι_{ir} are small positive constants.

Substituting (33) into (32), the time derivative of $\hat{\vartheta}_{ie}$ and $\hat{r}_{ie}$ can be denoted as

$$\begin{cases} \dot{\hat{\vartheta}}_{ie} = -k_{i1}^c \hat{\vartheta}_{ie} - k_{i2}^c \rho_{i\vartheta} - \gamma_{i3}\lceil \tilde{\vartheta}_i \rfloor^{\frac{1}{2}}, \\ \dot{\hat{r}}_{ie} = -k_{i3}^c \hat{r}_{ie} - k_{i4}^c \rho_{ir} - \gamma_{i5}\lceil \tilde{r}_i \rfloor^{\frac{1}{2}}. \end{cases} \tag{34}$$

3.3. Stability analysis

In the last parts, a finite-time leader–follower anti-disturbance synchronization controller has been devised. In this section, we aim to analyze the stability of the closed-loop system. Recall and summary the tracking error dynamics of x_{ie}, y_{ie}, ψ_{ie}, $\hat{\vartheta}_{ie}$ and $\hat{r}_{ie}$ as follows

$$\begin{cases} \dot{x}_{ie} = -k_{i1}^d x_{ie} - k_{i2}^d \rho_{ix} + \vartheta_{ie} + q_{i\vartheta} - \tilde{\vartheta}_{i0} + \omega_0(y_{ie} + \delta_{iy}), \\ \dot{y}_{ie} = -\underline{\vartheta}_i y_{ie} - \underline{\vartheta}_i k_{i3}^d \rho_{iy} + \varrho_i - \omega_0(x_{ie} + \delta_{ix}), \\ \dot{\psi}_{ie} = -k_{i4}^d \psi_{ie} - k_{i5}^d \rho_{i\psi} + r_{ie} + q_{ir}, \\ \dot{\hat{\vartheta}}_{ie} = -k_{i1}^c \hat{\vartheta}_{ie} - k_{i2}^c \rho_{i\vartheta} - \gamma_{i3}\lceil \tilde{\vartheta}_i \rfloor^{\frac{1}{2}} - x_{ie}, \\ \dot{\hat{r}}_{ie} = -k_{i3}^c \hat{r}_{ie} - k_{i4}^c \rho_{ir} - \gamma_{i5}\lceil \tilde{r}_i \rfloor^{\frac{1}{2}} - \psi_{ie}. \end{cases} \tag{35}$$

The stability of the closed-loop system (35) is given via the following theorem.

Theorem 1. *Consider multiple under-actuated marine vessels with dynamics (4) and (6), the RED-based velocity observer (10), the REDs (27), the disturbance observers (29), the FTLOS guidance law (21) and the nonlinear anti-disturbance control law (33). Under Assumption 1–3, all tracking errors of the proposed closed-loop system are ultimately uniformly bounded. Moreover, the leader–follower synchronization control for underway replenishment of multiple under-actuated vessels can be achieved in a finite time.*

Proof. Construct a Lyapunov function candidate as

$$V_2 = \frac{1}{2}\sum_{i=1}^{N}(x_{ie}^2 + y_{ie}^2 + \psi_{ie}^2 + \hat{\vartheta}_{ie}^2 + \hat{r}_{ie}^2). \tag{36}$$

Taking the time derivative of V_2 along (35), it renders that

$$\begin{aligned} \dot{V}_2 = \sum_{i=1}^{N}\Big(& -k_{i1}^d x_{ie}^2 - \underline{\vartheta}_i y_{ie}^2 - k_{i4}^d \psi_{ie}^2 - k_{i1}^c \hat{\vartheta}_{ie}^2 - k_{i3}^c \hat{r}_{ie}^2 - k_{i2}^d x_{ie}\rho_{ix} \\ & -\underline{\vartheta}_i k_{i3}^d y_{ie}\rho_{iy} - k_{i5}^d \psi_{ie}\rho_{i\psi} - k_{i2}^c \hat{\vartheta}_{ie}\rho_{i\vartheta} - k_{i4}^c \hat{r}_{ie}\rho_{ir} \\ & +x_{ie}(q_{i\vartheta} + \vartheta_{ie} - \tilde{\vartheta}_{i0} + \omega_0\delta_{iy}) + y_{ie}(\varrho_i - \omega_0\delta_{ix}) \\ & +\psi_{ie}(q_{ir} + r_{ie}) - \gamma_{i3}\hat{\vartheta}_{ie}\lceil \tilde{\vartheta}_i \rfloor^{\frac{1}{2}} - \gamma_{i5}\hat{r}_{ie}\lceil \tilde{r}_i \rfloor^{\frac{1}{2}} \Big). \end{aligned} \tag{37}$$

Since $\vartheta_{ie} = \hat{\vartheta}_{ie} - \tilde{\vartheta}_i$ and $r_{ie} = \hat{r}_{ie} - \tilde{r}_i$, we have

$$\begin{aligned}\dot{V}_2 = \sum_{i=1}^{N} \Big(&- k_{i1}^d x_{ie}^2 - \underline{\vartheta}_i y_{ie}^2 - k_{i4}^d \psi_{ie}^2 - k_{i1}^c \hat{\vartheta}_{ie}^2 - k_{i3}^c \hat{r}_{ie}^2 - k_{i2}^d x_{ie}\rho_{ix} \\ &-\underline{\vartheta}_i k_{i3}^d y_{ie}\rho_{iy} - k_{i5}^d \psi_{ie}\rho_{i\psi} - k_{i2}^c \hat{\vartheta}_{ie}\rho_{i\vartheta} - k_{i4}^c \hat{r}_{ie}\rho_{ir} \\ &+x_{ie}(q_{i\vartheta} + \hat{\vartheta}_{ie} - \tilde{\vartheta}_i - \tilde{\vartheta}_{i0} + \omega_0\delta_{iy}) + y_{ie}(\varrho_i - \omega_0\delta_{ix}) \\ &+\psi_{ie}(q_{ir} + \hat{r}_{ie} - \tilde{r}_i) - \gamma_{i3}\hat{\vartheta}_{ie}\lceil\tilde{\vartheta}_i\rfloor^{\frac{1}{2}} - \gamma_{i5}\hat{r}_{ie}\lceil\tilde{r}_i\rfloor^{\frac{1}{2}} \Big).\end{aligned} \tag{38}$$

Using Young's inequality, there are

$$x_{ie}\hat{\vartheta}_{ie} \le \frac{1}{2}(x_{ie}^2 + \hat{\vartheta}_{ie}^2) \text{ and } \psi_{ie}\hat{r}_{ie} \le \frac{1}{2}(\psi_{ie}^2 + \hat{r}_{ie}^2). \tag{39}$$

According to Lemmas 3–4, we substitute (39) into (38) and rewrite $\dot{V}_2$ as

$$\begin{aligned}\dot{V}_2 \le \sum_{i=1}^{N} \Big(&- k_{i1}^{d'} x_{ie}^2 - \underline{\vartheta}_i y_{ie}^2 - k_{i4}^{d'} \psi_{ie}^2 - k_{i1}^{c'} \hat{\vartheta}_{ie}^2 - k_{i3}^{c'} \hat{r}_{ie}^2 - k_{i2}^d x_{ie}\rho_{ix} \\ &-\underline{\vartheta}_i k_{i3}^d y_{ie}\rho_{iy} - k_{i5}^d \psi_{ie}\rho_{i\psi} - k_{i2}^c \hat{\vartheta}_{ie}\rho_{i\vartheta} - k_{i4}^c \hat{r}_{ie}\rho_{ir} \\ &+|x_{ie}|(\bar{q}_{i\vartheta} + \bar{\vartheta}_i + \bar{\vartheta}_{i0} + \bar{\omega}_0|\delta_{iy}|) + |y_{ie}|(\bar{\varrho}_i + \bar{\omega}_0|\delta_{ix}|) \\ &+|\psi_{ie}|(\bar{q}_{ir} + \bar{r}_i) + \gamma_{i3}|\hat{\vartheta}_{ie}||\tilde{\vartheta}_i|^{\frac{1}{2}} + \gamma_{i5}|\hat{r}_{ie}||\tilde{r}_i|^{\frac{1}{2}} \Big),\end{aligned} \tag{40}$$

with $k_{i1}^{d'} = k_{i1}^d - \frac{1}{2}$, $k_{i4}^{d'} = k_{i4}^d - \frac{1}{2}$, $k_{i1}^{c'} = k_{i1}^c - \frac{1}{2}$ and $k_{i3}^{c'} = k_{i3}^c - \frac{1}{2}$.

Define the variables $h_{i1} = \min\{k_{i1}^{d'}, \underline{\vartheta}_i, k_{i4}^{d'}, k_{i1}^{c'}, k_{i3}^{c'}\}$, $h_{i2} = \min\{k_{i2}^d, \underline{\vartheta}_i k_{i3}^d, k_{i5}^d, k_{i2}^c, k_{i4}^c\}$, $h_{i3} = \max\{h_{ix}, h_{iy}, h_{i\psi}, h_{i\vartheta}, h_{ir}\}$ with $h_{ix} = \bar{q}_{i\vartheta} + \bar{\vartheta}_i + \bar{\vartheta}_{i0} + \bar{\omega}_0|\delta_{iy}|$; $h_{iy} = \bar{\varrho}_i + \bar{\omega}_0|\delta_{ix}|$; $h_{i\psi} = \bar{q}_{ir} + \bar{\vartheta}_i$; $h_{i\vartheta} = \gamma_{i3}|\tilde{\vartheta}_i|^{\frac{1}{2}}$ and $h_{ir} = \gamma_{i5}|\tilde{r}_i|^{\frac{1}{2}}$. Then, it implies that

$$\begin{aligned}\dot{V}_2 \le \sum_{i=1}^{N} \Big(&-h_{i1}(x_{ie}^2 + y_{ie}^2 - k_{i4}^{d'}\psi_{ie}^2 + \hat{\vartheta}_{ie}^2 + \hat{r}_{ie}^2) - h_{i2}(x_{ie}\rho_{ix} + y_{ie}\rho_{iy} + \\ &\psi_{ie}\rho_{i\psi} + \hat{\vartheta}_{ie}\rho_{i\vartheta} + \hat{r}_{ie}\rho_{ir}) + h_{i3}(|x_{ie}| + |y_{ie}| + |\psi_{ie}| + |\hat{\vartheta}_{ie}| + |\hat{r}_{ie}|) \Big),\end{aligned} \tag{41}$$

To simplify the process, we define the vectors $x_e = [x_{1e}, \dots, x_{Ne}]^T$, $y_e = [y_{1e}, \dots, y_{Ne}]^T$, $\psi_e = [\psi_{1e}, \dots, \psi_{Ne}]^T$, $\hat{\vartheta}_e = [\hat{\vartheta}_{1e}, \dots, \hat{\vartheta}_{Ne}]^T$, $\hat{r}_e = [\hat{r}_{1e}, \dots, \hat{r}_{Ne}]^T$, $\rho_x = [\rho_{1x}, \dots, \rho_{Nx}]^T$, $\rho_y = [\rho_{1y}, \dots, \rho_{Ny}]^T$, $\rho_\psi = [\rho_{1\psi}, \dots, \rho_{N\psi}]^T$, $\rho_\vartheta = [\rho_{1\vartheta}, \dots, \rho_{N\vartheta}]^T$, $\rho_r = [\rho_{1r}, \dots, \rho_{Nr}]^T$. Thus, $\dot{V}_2$ can be further represented as

$$\begin{aligned}\dot{V}_2 \le &- h_1 \left(\|x_e\|^2 + \|y_e\|^2 + \|\psi_e\|^2 + \|\hat{\vartheta}_e\|^2 + \|\hat{r}_e\|^2\right) \\ &- h_2 \left(x_e^T\rho_x + y_e^T\rho_y + \psi_e^T\rho_\psi + \hat{\vartheta}_e^T\rho_\vartheta + \hat{r}_e^T\rho_r\right) \\ &+ h_3 \left(\|x_e\| + \|y_e\| + \|\psi_e\| + \|\hat{\vartheta}_e\| + \|\hat{r}_e\|\right),\end{aligned} \tag{42}$$

where $h_1 = \min_{i=1,\dots,N}\{h_{i1}\}$, $h_2 = \min_{i=1,\dots,N}\{h_{i2}\}$, and $h_3 = \min_{i=1,\dots,N}\{h_{i3}\}$.

Letting $E_1 = [x_e^T,\ y_e^T,\ \psi_e^T,\ \hat{\vartheta}_e^T,\ \hat{r}_e^T]^T$ and $E_2 = [\rho_x^T, \rho_y^T, \rho_\psi^T, \rho_\vartheta^T, \rho_r^T]^T$, one has

$$\dot{V}_2 \le -h_1\|E_1\|^2 - h_2 E_1^T E_2 + h_3\|E_1\|. \tag{43}$$

According to the definition of ρ_{ix}, ρ_{iy}, $\rho_{i\psi}$, $\rho_{i\vartheta}$, and ρ_{ir}, the following discussion is needed.

Case 1: When $|x_{ie}| < \iota_{ix}$, $|y_{ie}| < \iota_{iy}$, $|\psi_{ie}| < \iota_{i\psi}$, $|\hat{\vartheta}_{ie}| < \iota_{i\vartheta}$ and $|\hat{r}_{ie}| < \iota_{ir}$, $i = 1, \dots, N$, it gets $E_2 = \iota E_1$ with $\iota = \mathrm{diag}\{\iota_{1x}, \dots, \iota_{Nx}, \iota_{1y}, \dots, \iota_{Ny}, \iota_{1\psi}, \dots, \iota_{N\psi}, \iota_{1\vartheta}, \dots, \iota_{N\vartheta}, \iota_{1r}, \dots, \iota_{Nr}\}$. Then it yields

$$\dot{V}_2 \le -\left(h_1 + h_2\lambda_{\min}(\iota)\right)\|E_1\|^2 + h_3\|E_1\| \tag{44}$$

For $\|E_1\| \ge h_3/(\theta c_1)$ with $c_1 = h_1 + h_2\lambda_{\min}(\iota)$ and $0 < \theta < 1$, the derivative of V_2 can be expressed as

$$\dot{V}_2 \le -c_1(1-\theta)\|E_1\|^2. \tag{45}$$

Thus, all error signals of the closed system (35) are uniformly ultimately bounded when $|x_{ie}| < \iota_{ix}$, $|y_{ie}| < \iota_{iy}$, $|\psi_{ie}| < \iota_{i\psi}$, $|\hat{\vartheta}_{ie}| < \iota_{i\vartheta}$ and $|\hat{r}_{ie}| < \iota_{ir}$, $i = 1, \dots, N$.

Case 2: When $|x_{ie}| \ge \iota_{ix}$, $|y_{ie}| \ge \iota_{iy}$, $|\psi_{ie}| \ge \iota_{i\psi}$, $|\hat{\vartheta}_{ie}| \ge \iota_{i\vartheta}$ and $|\hat{r}_{ie}| \ge \iota_{ir}$, $i = 1, \dots, N$, it gets $E_2 = \lceil E_1\rfloor^{\frac{1}{2}}$. Substituting E_2 into (43), we have

$$\dot{V}_2 \le -h_1\|E_1\|^2 - h_2\|E_1\|^{\frac{3}{2}} + h_3\|E_1\|. \tag{46}$$

From (46), we can further obtain two inequalities as

$$\dot{V}_2 \le -\left(h_1 - h_3/\|E_1\|\right)\|E_1\|^2 - h_2\|E_1\|^{\frac{3}{2}} \tag{47}$$

and

$$\dot{V}_2 \le -h_1\|E_1\|^2 - \left(h_2 - h_3/\|E_1\|^{\frac{1}{2}}\right)\|E_1\|^{\frac{3}{2}}. \tag{48}$$

Based on the inequality (47), for $\|E_1\| > h_3/h_1$, it implies that

$$\dot{V}_2 \le -c_2 V_2 - c_3 V_2^{\frac{3}{4}}, \tag{49}$$

where $c_2 = h_1 - h_3/\|E_1\|$ and $c_3 = h_2$.

According to Lemma 2, the region $\|E_1\| \le h_3/h_1$ can be arrived in a finite time t_1 satisfying

$$t_1 \le t_0 + \frac{4\|E_1\|}{h_1\|E_1\| - h_3} \ln\left(\frac{(h_1\|E_1\| - h_3)V_2^{\frac{1}{4}}(t_0) + c_3\|E_1\|}{c_3\|E_1\|}\right).$$

Based on (48), when $\|\Xi\| > \left(h_3^2/h_2^2\right)$, $\dot{V}_2$ can be devised as

$$\dot{V}_2 \le -c_4 V_2 - c_5 V_2^{\frac{3}{4}} \tag{50}$$

with $c_4 = h_1$ and $c_5 = h_2 - h_3/\|E_1\|^{\frac{1}{2}}$.

Using Lemma 2, the region $\|E_1\| \le \left(h_3^2/h_2^2\right)$ is reached in a finite time t_2 satisfying

$$t_2 \le t_0 + \frac{4}{h_1} \ln\left(\frac{h_1\|E_1\|^{\frac{1}{2}} V_2^{\frac{1}{4}}(t_0) + h_2\|E_1\|^{\frac{1}{2}} - h_3}{h_2\|E_1\|^{\frac{1}{2}} - h_3}\right).$$

Therefore, it is concluded that E_1 in this case is bounded and satisfied with

$$\|E_1\| \le \min\left\{\frac{h_3}{h_1}, \frac{h_3^2}{h_2^2}\right\} \tag{51}$$

in a finite time $T_2 \le \max\{t_1, t_2\}$. The proof is completed. □

4. Simulation results

In this section, a simulation example is used to illustrate the effectiveness of the proposed finite-time anti-disturbance synchronization control method. Consider an underway replenished system with a leader vessel and two under-actuated follower marine vessels.

This simulation adapts the under-actuated vessel model in Skjetne et al. (2005). The initial state of two follower vessels are predefined as $(x_1, y_1, \psi_1, u_1, v_1, r_1) = (4, -8, \pi/2, 0, 0, 0)$, $(x_2, y_2, \psi_2, u_2, v_2, r_2) = (-8, 3, 0, 0, 0, 0)$. The leader vessel is driven to move along a given trajectory $p(t) = [x(t), y(t)]^T = [\sqrt{2}t/4, \sqrt{2}t/4]^T$, $t \ge 0$. The initial position and heading of leader vessel is set as $(x_0, y_0, \psi_0) = (0, 0, \pi/4)$. The proposed control laws in last section are summarized in Table 1. The corresponding parameters for the proposed observers and controllers are listed in Table 2. In order to show that FTLOS guidance law has a faster convergence ability, a non-finite time LOS guidance (Gu et al., 2019) is used to compare with the FTLOS. For $t > 80$, we increase the environmental disturbance to demonstrate the robustness of the proposed method.

The simulation results are given in Figs. 3–9. Specially, Fig. 3 presents the actual trajectories of the leader and follower marine vessels guided by the proposed FTLOS guidance law (21) and nonlinear control law (33). Fig. 4 provides along-tracking errors and cross-tracking errors of the follower vessels guided by FTLOS and LOS. From Fig. 4, we know that the FTLOS-guided follower vessels can converge to the reference point in a shorter time. According to Figs. 3 and 4, the proposed FTLOS method still enables the underactuated vessels to hold the better

Table 1
Anti-disturbance synchronization control algorithm.

Kinematic level	
Velocity observer	$\dot{\hat{x}}_{ie} = -\gamma_{i1}\lceil \hat{x}_{ie} - x_{ie}\rfloor^{\frac{1}{2}} + \hat{\vartheta}_{i0} + \vartheta_i \cos(\psi_i - \psi_0) + \omega_0(y_{ie} + \delta_{iy})$ $\dot{\hat{\vartheta}}_{i0} = -\gamma_{i2}\lceil \hat{x}_{ie} - x_{ie}\rfloor^{0}$
FTLOS guidance law	$\alpha_{i\vartheta} = -k^d_{i1}x_{ie} - k^d_{i2}\rho_{ix} + 2\vartheta_i \sin^2\left(\frac{\psi_i-\psi_0}{2}\right) - \hat{\vartheta}_{i0}$ $\alpha_{i\psi} = \mathrm{atan2}\left(-\frac{y_{ie}+k^d_{i3}\rho_{iy}}{\Delta_i}\right) + \psi_0 - \beta_i$ $\alpha_{ir} = -k^d_{i4}\psi_{ie} - k^d_{i5}\rho_{i\psi} - \beta_{id} + \dot{\alpha}_{i\psi}$
Kinetic level	
Differentiators	$\dot{\vartheta}_{if} = -\gamma^{\vartheta}_{i1}\lceil \vartheta_{if} - \alpha_{i\vartheta}\rfloor^{\frac{1}{2}} + \vartheta^d_{if}$ $\dot{\vartheta}^d_{if} = -\gamma^{\vartheta}_{i2}\lceil \vartheta_{if} - \alpha_{i\vartheta}\rfloor^{0}$ $\dot{r}_{if} = -\gamma^{r}_{i1}\lceil r_{if} - \alpha_{ir}\rfloor^{\frac{1}{2}} + r^d_{if}$ $\dot{r}^d_{if} = -\gamma^{r}_{i2}\lceil r_{if} - \alpha_{ir}\rfloor^{0}$
Disturbance observers	$\dot{\hat{\vartheta}}_i = -\gamma_{i3}\lceil \hat{\vartheta}_i - \vartheta_i\rfloor^{\frac{1}{2}} + \hat{\sigma}_{i\vartheta} + m^{-1}_{iu}\tau_{iu}$ $\dot{\hat{\sigma}}_{i\vartheta} = -\gamma_{i4}\lceil \hat{\vartheta}_i - \vartheta_i\rfloor^{0}$ $\dot{\hat{r}}_i = -\gamma_{i5}\lceil \hat{r}_i - r_i\rfloor^{\frac{1}{2}} + \hat{\sigma}_{ir} + m^{-1}_{ir}\tau_{ir}$ $\dot{\hat{\sigma}}_{ir} = -\gamma_{i6}\lceil \hat{r}_i - r_i\rfloor^{0}$
Nonlinear control law	$\tau_{iu} = m_{iu}(-k^c_{i1}\hat{\vartheta}_{ie} - k^c_{i2}\rho_{i\vartheta} - \hat{\sigma}_{i\vartheta} + \dot{\vartheta}_{if})$ $\tau_{ir} = m_{ir}(-k^c_{i3}\hat{r}_{ie} - k^c_{i4}\rho_{ir} - \hat{\sigma}_{ir} + \dot{r}_{if})$

Table 2
The parameters of observers and controllers in the simulation.

Kinematic level								
Parameter	γ_{i1}	γ_{i2}	k^d_{i1}	k^d_{i2}	k^d_{i3}	k^d_{i4}	k^d_{i5}	Δ_i
Value	2.0	0.40	0.05	0.10	1	0.15	0.25	5
Parameter	δ_{1x}	δ_{2x}	δ_{1y}	δ_{2y}	ι_{ix}	ι_{iy}	$\iota_{i\psi}$	
Value	0	0	4	−4	0.2	0.5	0.1	
Kinetic level								
Parameter	γ^{ϑ}_{i1}	γ^{ϑ}_{i2}	γ^{r}_{i1}	γ^{r}_{i2}	γ_{i3}	γ_{i4}	γ_{i5}	γ_{i6}
Value	2.5	0.25	2.5	0.25	8.0	5.0	2.5	1.2
Parameter	k^c_{i1}	k^c_{i2}	k^c_{i3}	k^c_{i4}	ι_{iy}	$\iota_{i\psi}$		
Value	1.2	0.2	2.0	0.25	0.001	0.001		

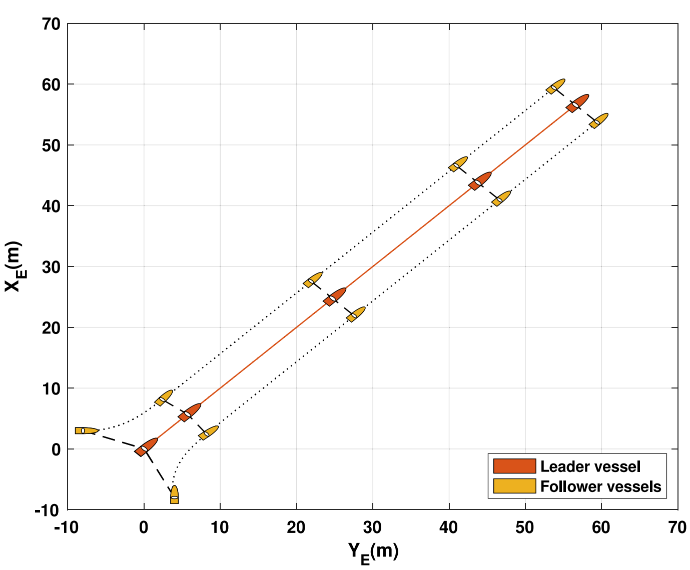

Fig. 3. The trajectory of the leader and follower marine vessels.

tracking performance when the environmental disturbances increase. In the first subplot of Fig. 5, the desired and actual heading of the follower vessels are depicted by considering the time-varying slide-angle. In the second one of Fig. 5, the actual total velocity of the leader vessel is recovered by the designed observer (10) for each follower vessel. Fig. 6

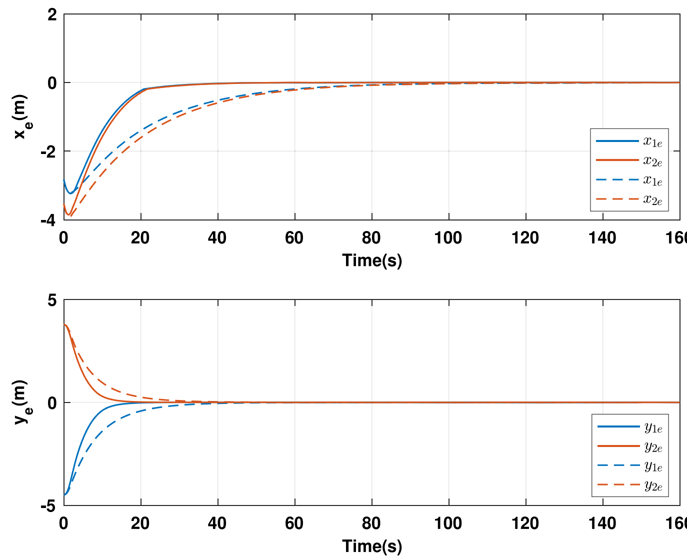

Fig. 4. The along-track and cross-track errors of follower marine vessels (solid line: FTLOS; dash line: LOS).

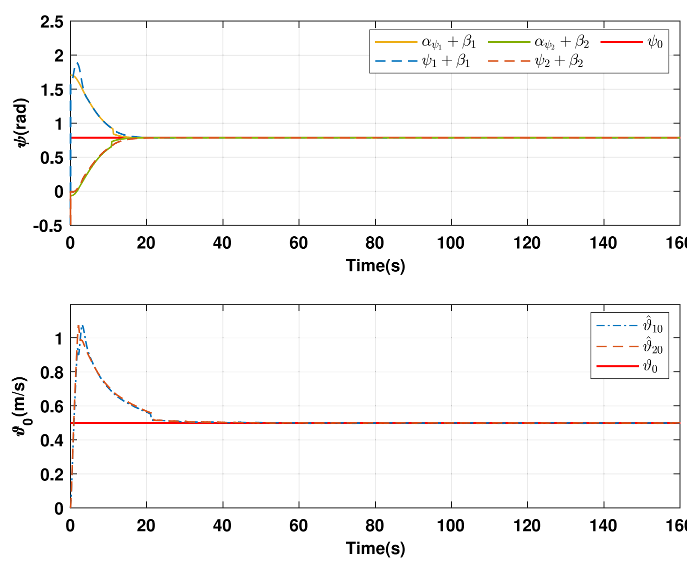

Fig. 5. The cross-track errors of the follower marine vessels.

displays the desired total velocity from (21), the estimated desired total velocity from (27), actual total velocity and the estimated total velocity from (29). Fig. 7 displays the desired angular velocity by (21), the estimated desired angular velocity by (27), actual angular velocity and the estimated angular velocity by (29). Under the environmental disturbances, follower vessels can achieve convergence of the cross-tracking errors via adjusting heading. Fig. 8 depicts the actual and estimated total uncertainties from the proposed disturbance observer (29) in ϑ direction. Similarly, Fig. 9 shows the actual and the estimated total uncertainties from the proposed disturbance observer (29) in r direction. Fig. 10 describes the surge force τ_{iu} and the yaw moment τ_{ir} during the whole process.

5. Conclusion

In this paper, an anti-disturbance leader–follower synchronization control method based on REDs is proposed for underway replenishment of multiple under-actuated marine vessels subject to unknown model uncertainties and external disturbances. The architecture of the

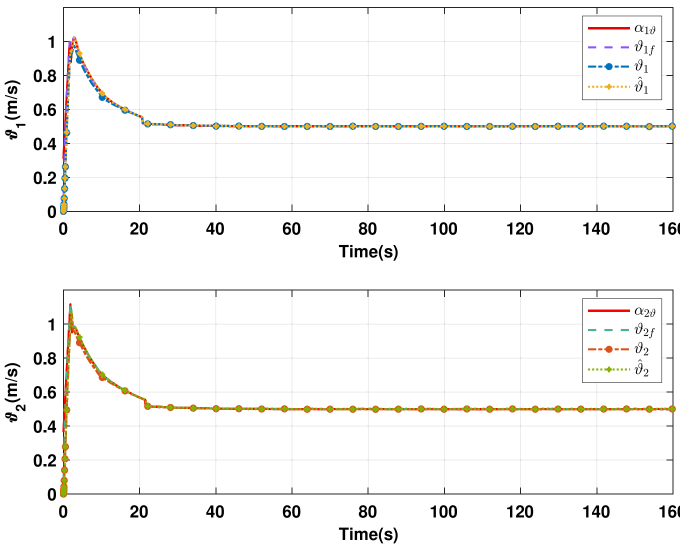

Fig. 6. The total velocity signals of the follower marine vessels.

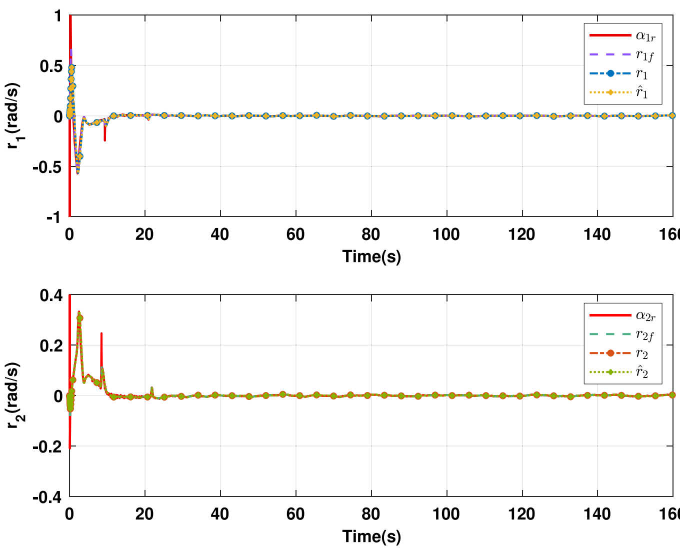

Fig. 7. The yaw angular velocity signals in u direction.

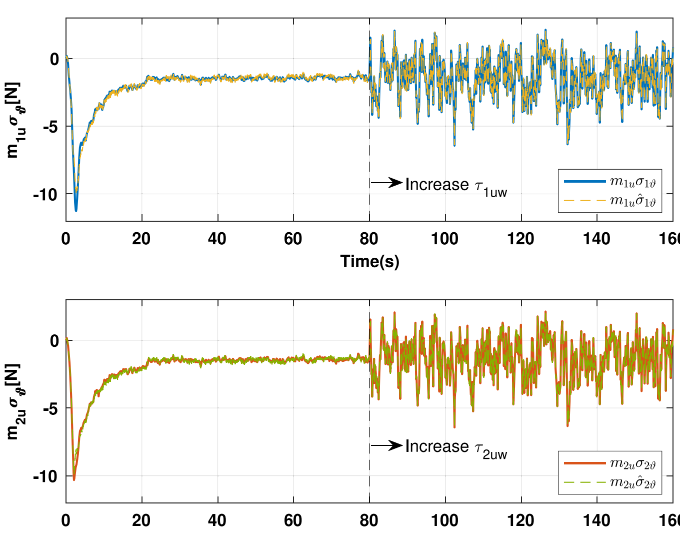

Fig. 8. The estimations of total uncertainties in ϑ direction.

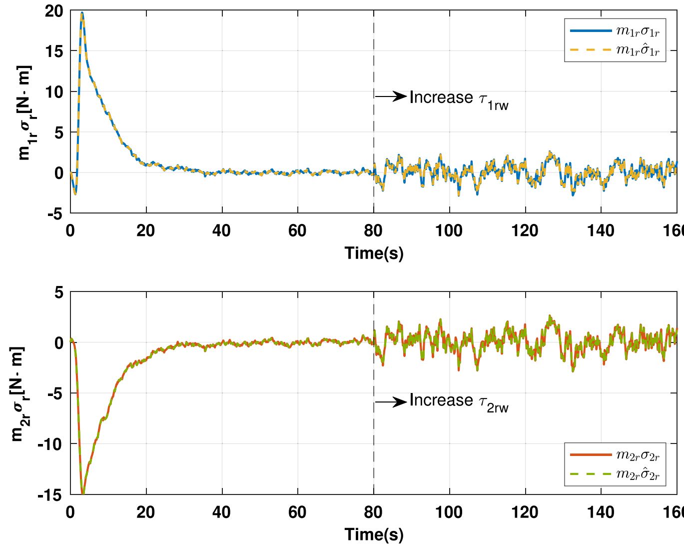

Fig. 9. The estimations of total uncertainties in r direction.

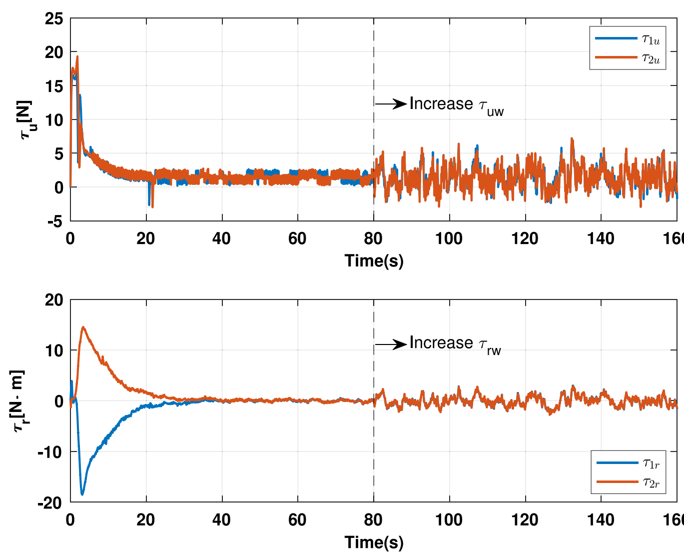

Fig. 10. The surge force and yaw moment of the follower marine vessels.

proposed closed-loop system can be divided into a kinematic loop and a kinetic loop. Specifically, at the kinematic level, the RED-based observer can estimate the unknown total velocity of the leader vessel. With the estimated velocity, the proposed FTLOS guidance law can provide the desired synchronization commands for multiple under-actuated marine vessels. Next, at the kinetic level, two REDs can be used to smooth the signals from the kinematic loop. The unknown model uncertainties and disturbances due to wind, wave and current can be exactly estimated via the proposed disturbance observers. Based on the estimation, the proposed nonlinear anti-disturbance control law can track robustly the desired signals. Then, the stability of the closed-loop system is analyzed by a Lyapunov stability theory and all errors are ultimately uniformly bounded. Finally, the effectiveness of the proposed anti-disturbance synchronization control method for marine vessels is illustrated via a simulation example.

CRediT authorship contribution statement

Wentao Wu: Software, Validation, Writing – original draft, Visualization, Writing – review & editing, Data curation, Project administration. **Zhouhua Peng:** Supervision, Conceptualization, Funding acquisition, Project administration, Methodology, Investigation. **Dan Wang:** Supervision, Methodology, Investigation, Resources, Project administration. **Lu Liu:** Funding acquisition, Project administration. **Nan Gu:** Methodology, Investigation.

Declaration of competing interest

The authors declare that they have no known competing financial interests or personal relationships that could have appeared to influence the work reported in this paper.

Acknowledgments

This work was supported in part by the National Natural Science Foundation of China under Grants 51979020, 51909021, 51939001, 52071044, and in part by the Top-notch Young Talents Program of China, and in part by the Liaoning Revitalization Talents Program, China under Grant XLYC2007188, and in part by Science and Technology Fund for Distinguished Young Scholars of Dalian, China under Grant 2018RJ08, and in part by the Fundamental Research Funds for the Central Universities, China under Grant 3132019319, and in part by the Hainan Special PhD Scientific Research Foundation of Sanya Yazhou Bay Science and Technology City under Grant HSPHDSRF-2022-01-007.

References

Belleter, D.J.W., Pettersen, K.Y., 2017. Leader–follower synchronisation for a class of underactuated systems. Nonlinear Syst.: Tech. Dyn. Anal. Control 157–179.

Bondhus, A.K., Pettersen, K.Y., 2005. Control of ship replenishment by output feedback synchronization. In: Proceedings of OCEANS 2005 MTS/IEEE, Vol. 2, pp. 1610–1617.

Breivik, M., Hovstein, V.E., Fossen, T.I., 2008. Straight-line target tracking for unmanned surface vehicles. Model. Identif. Control 29 (4), 131–149.

Chu, Z., Xiang, X., Zhu, D., Luo, C., Xie, D., 2017. Adaptive fuzzy sliding mode diving control for autonomous underwater vehicle with input constraint. Int. J. Fuzzy Syst. 20 (5), 1460–1469.

Cui, R., Chen, L., Yang, C., Chen, M., 2017. Extended state observer-based integral sliding mode control for an underwater robot with unknown disturbances and uncertain nonlinearities. IEEE Trans. Ind. Electron. 64 (8), 6785–6795.

Cui, R., Yan, W., Xu, D., 2012. Synchronization of multiple autonomous underwater vehicles without velocity measurements. Sci. China Inf. Sci. 55 (7), 1693–1703.

Dai, S., Wang, C., Luo, F., 2012. Identification and learning control of ocean surface ship using neural networks. IEEE Trans. Ind. Inform. 8 (4), 801–810.

Davila, A., Moreno, J., Fridman, L., 2009. Optimal Lyapunov function selection for reaching time estimation of Super Twisting algorithm. In: Proceedings of the 48th IEEE Conference on Decision and Control, 2009, pp. 8405–8410.

Fossen, T.I., 2011. Handbook of Marine Craft Hydrodynamics and Motion Control. John Wiley & Sons.

Gierusz, W., Miller, A., 2016. Ship motion control system for replenishment operation. Appl. Mech. Mater. 817, 214–222.

Gu, N., Peng, Z., Wang, D., Shi, Y., Wang, T., 2019. Antidisturbance coordinated path following control of robotic autonomous surface vehicles: Theory and experiment. IEEE/ASME Trans. Mechatronics 24 (5), 2386–2396.

Gu, N., Wang, D., Peng, Z., Liu, L., 2020. Adaptive bounded neural network control for coordinated path-following of networked underactuated autonomous surface vehicles under time-varying state-dependent cyber-attack. ISA Trans. 104, 212–221.

Guo, Y., Qin, H., Xu, B., Han, Y., Fan, Q.-Y., Zhang, P., 2019. Composite learning adaptive sliding mode control for AUV target tracking. Neurocomputing (ISSN: 0925-2312) 351, 180–186.

Guo, B., Wu, Z., Zhou, H., 2016. Active disturbance rejection control approach to output-feedback stabilization of a class of uncertain nonlinear systems subject to stochastic disturbance. IEEE Trans. Autom. Control 61 (6), 1613–1618.

He, S., Dai, S., Dong, C., 2022. Adaptive synchronization control of uncertain multiple USVs with prescribed performance and preserved connectivity. Sci. China Inf. Sci. 65 (9), 1–2.

He, S., Wang, M., Dai, S., Luo, F., 2019. Leader-follower formation control of USVs with prescribed performance and collision avoidance. IEEE Trans. Ind. Inf. 15 (1), 572–581.

Hong, Y., Huang, J., Xu, Y., 2001. On an output feedback finite-time stabilization problem. IEEE Trans. Automat. Control 46 (2), 305–309.

Ihle, I.-A.F., Arcak, M., Fossen, T.I., 2007. Passivity-based designs for synchronized path-following. Automatica 43 (9), 1508–1518.

Jin, X., 2016. Fault tolerant finite-time leader–follower formation control for autonomous surface vessels with LOS range and angle constraints. Automatica 68, 228–236.

Jin, X., 2018. Adaptive fixed-time control for MIMO nonlinear systems with asymmetric output constraints using universal barrier functions. IEEE Trans. Automat. Control 64 (7), 3046–3053.

Kyrkjebø, E., 2007. Motion coordination of mechanical systems: leader-follower synchronization of Euler-Lagrange systems using output feedback control.

Kyrkjebø, E., 2015. Dynamic and kinematic observers for output coordination control of Euler-Lagrange systems: A comparison and applications. Model. Identif. Control: Nor. Res. Bull. 36, 103–118.

Kyrkjebø, E., Pettersen, K.Y., Wondergem, M., Nijmeijer, H., 2007. Output synchronization control of ship replenishment operations: Theory and experiments. Control Eng. Pract. (ISSN: 0967-0661) 15 (6), 741–755.

Levant, A., 1998. Robust exact differentiation via sliding mode technique. Automatica 34 (3), 379–384.

Liu, B., Chen, Z., Zhang, H., Wang, X., Geng, T., Su, H., Zhao, J., 2020a. Collective dynamics and control for multiple unmanned surface vessels. IEEE Trans. Control Syst. Technol. 28 (6), 2540–2547.

Liu, Y., Du, J., Hu, X., 2018a. Synchronisation control for ships in underway replenishment based on dynamic surface control. Int. J. Autom. Control 12 (2), 220–236.

Liu, L., Wang, D., Peng, Z., 2017. ESO-based line-of-sight guidance law for path following of underactuated marine surface vehicles with exact sideslip compensation. IEEE J. Ocean. Eng. 42 (2), 477–487.

Liu, L., Wang, D., Peng, Z., Chen, C.L.P., Li, T., 2019. Bounded neural network control for target tracking of underactuated autonomous surface vehicles in the presence of uncertain target dynamics. IEEE Trans. Neural Netw. Learn. Syst. 30, 1241–1249.

Liu, L., Wang, D., Peng, Z., Li, T., Chen, C.L.P., 2020b. Cooperative path following ring-networked under-actuated autonomous surface vehicles: Algorithms and experimental results. IEEE Trans. Cybern. 50 (4), 1519–1529.

Liu, L., Wang, D., Peng, Z., Wang, H., 2016. Predictor-based LOS guidance law for path following of underactuated marine surface vehicles with sideslip compensation. Ocean Eng. 124, 340–348.

Liu, Z., Wang, Y., Wang, T., 2018b. Incremental predictive control-based output consensus of networked unmanned surface vehicle formation systems. Inform. Sci. 457–458, 166–181.

Lu, Y., Zhang, G., Qiao, L., Zhang, W., 2020. Adaptive output-feedback formation control for underactuated surface vessels. Internat. J. Control 93 (3), 400–409.

Lu, Y., Zhang, G., Sun, Z., Zhang, W., 2018. Adaptive cooperative formation control of autonomous surface vessels with uncertain dynamics and external disturbances. Ocean Eng. (ISSN: 0029-8018) 167, 36–44.

Moulay, E., Perruquetti, W., 2006. Finite time stability and stabilization of a class of continuous systems. J. Math. Anal. Appl. 323 (2), 1430–1443.

Peng, Z., Gu, N., Zhang, Y., Liu, Y., Wang, D., Liu, L., 2019. Path-guided time-varying formation control with collision avoidance and connectivity preservation of underactuated autonomous surface vehicles subject to unknown input gains. Ocean Eng. 191, 106501.

Peng, Z., Jiang, Y., Wang, J., 2021. Event-triggered dynamic surface control of an underactuated autonomous surface vehicle for target enclosing. IEEE Trans. Ind. Electron. 68 (4), 3402–3412.

Peng, Z., Wang, D., Chen, Z., Hu, X., Lan, W., 2013. Adaptive dynamic surface control for formations of autonomous surface vehicles with uncertain dynamics. IEEE Trans. Control Syst. Technol. 21 (2), 513–520.

Peng, Z., Wang, D., Li, T., Han, M., 2020. Output-feedback cooperative formation maneuvering of autonomous surface vehicles with connectivity preservation and collision avoidance. IEEE Trans. Cybern. 50 (6), 2527–2535.

Qin, H., Li, C., Sun, Y., Wang, N., 2020. Adaptive trajectory tracking algorithm of unmanned surface vessel based on anti-windup compensator with full-state constraints. Ocean Eng. 200, 106906.

Skejic, R., Breivik, M., Fossen, T.I., Faltinsen, O.M., 2009. Modeling and control of underway replenishment operations in calm water. IFAC Proc. Vol. 42 (18), 78–85.

Skjetne, R., Fossen, T.I., Kokotović, P.V., 2005. Adaptive maneuvering, with experiments, for a model ship in a marine control laboratory. Automatica 41 (2), 289–298.

Wang, Y., Han, Q., 2017. Network-based heading control and rudder oscillation reduction for unmanned surface vehicles. IEEE Trans. Control Syst. Technol. 25, 1609–1620.

Wu, W., Peng, Z., Wang, D., Liu, L., Han, Q.-L., 2021. Network-based line-of-sight path tracking of underactuated unmanned surface vehicles with experiment results. IEEE Trans. Cybern. 1–11.

Xiang, X., Yu, C., Zhang, Q., 2017. Robust fuzzy 3D path following for autonomous underwater vehicle subject to uncertainties. Comput. Oper. Res. 84, 165–177.

Zhang, G., Deng, Y., Zhang, W., 2017. Robust neural path-following control for underactuated ships with the DVS obstacles avoidance guidance. Ocean Eng. 143, 198–208.

Zheng, Z., Sun, L., Xie, L., 2018. Error-constrained LOS path following of a surface vessel with actuator saturation and faults. IEEE Trans. Syst. Man Cybern.: Syst. 48 (10), 1794–1805.

Zheng, Z., Zou, Y., 2016. Adaptive integral LOS path following for an unmanned airship with uncertainties based on robust RBFNN backstepping. ISA Trans. 65, 210–219.